

A high-strength Sm-doped CeO₂ oxide-ion conducting electrolyte membrane for solid oxide fuel cell application

Yingchao Dong ^{a,b}, Dongfeng Li ^b, Xuyong Feng ^a, Xinfu Dong ^c, Stuart Hampshire ^{b*}

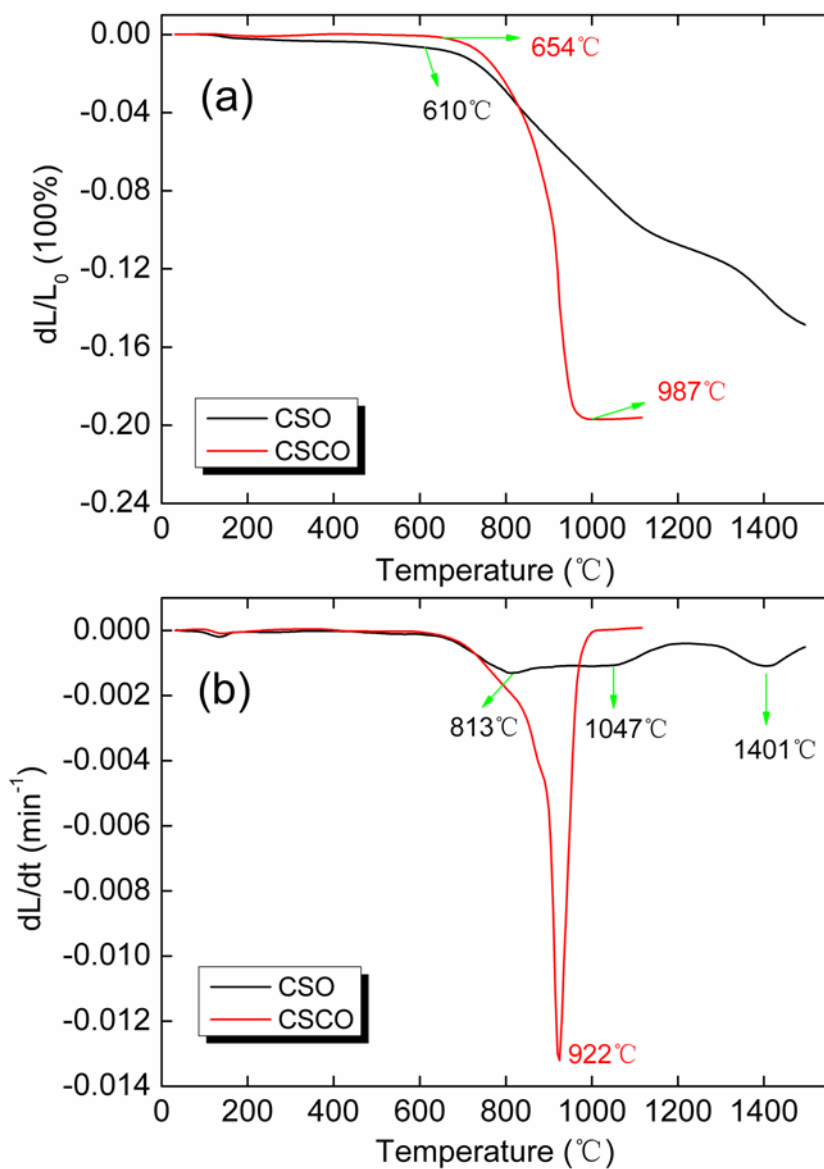


Fig. S1. Linear shrinkage dL/L_0 (a) and differential linear shrinkage dL/dt (b) of the CSO and CSCO samples.

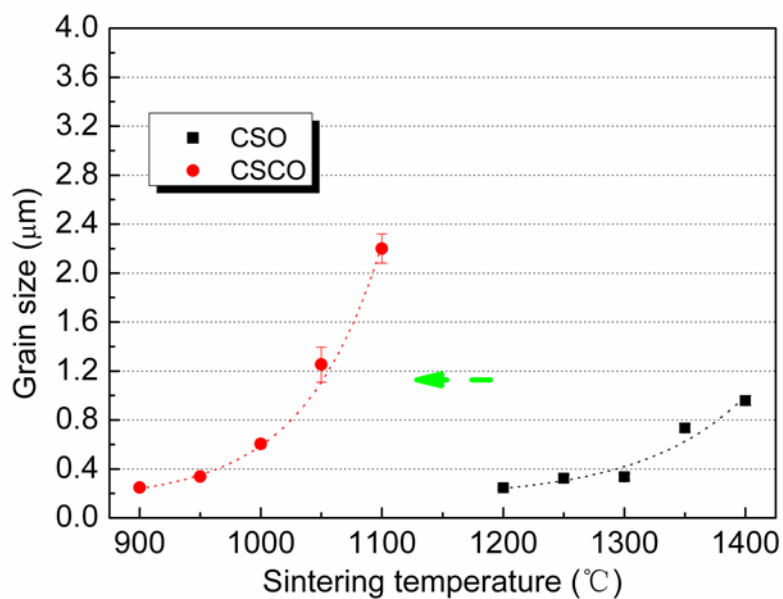


Fig. S2. Grain size of the CSO and CSCO sintered bodies at different temperatures.

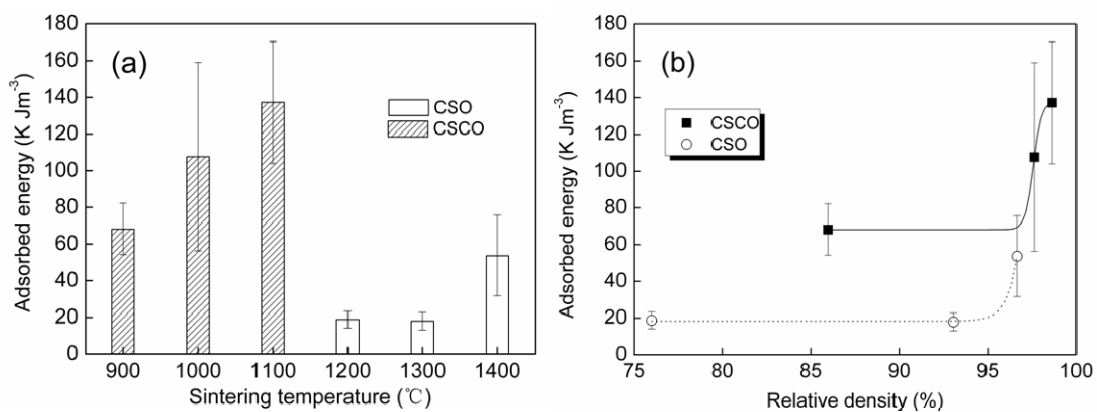


Fig. S3. Fracture adsorbed energies of the CSO and CSCO sintered bodies at different sintering temperatures (a)

and at different relative densities (b).

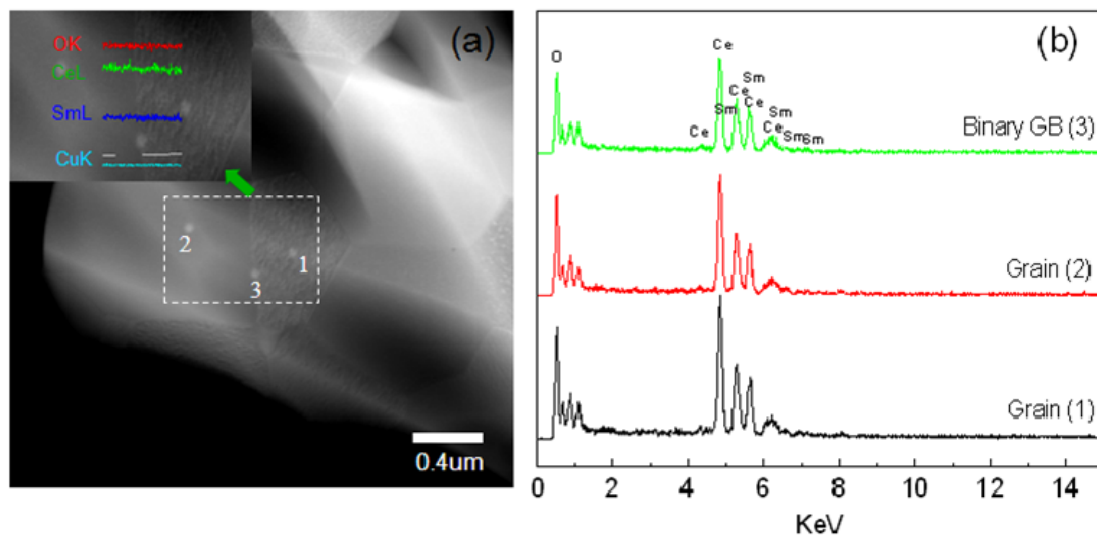


Fig. S4. STEM-EDS results for CSO-1400: (a) STEM image (the insert shows a STEM enlarged image and EDS element linear scanning results across a binary grain boundary between two typical grains); (b) EDS spectra of Grain (1), Grain (2) and binary grain boundary (3).

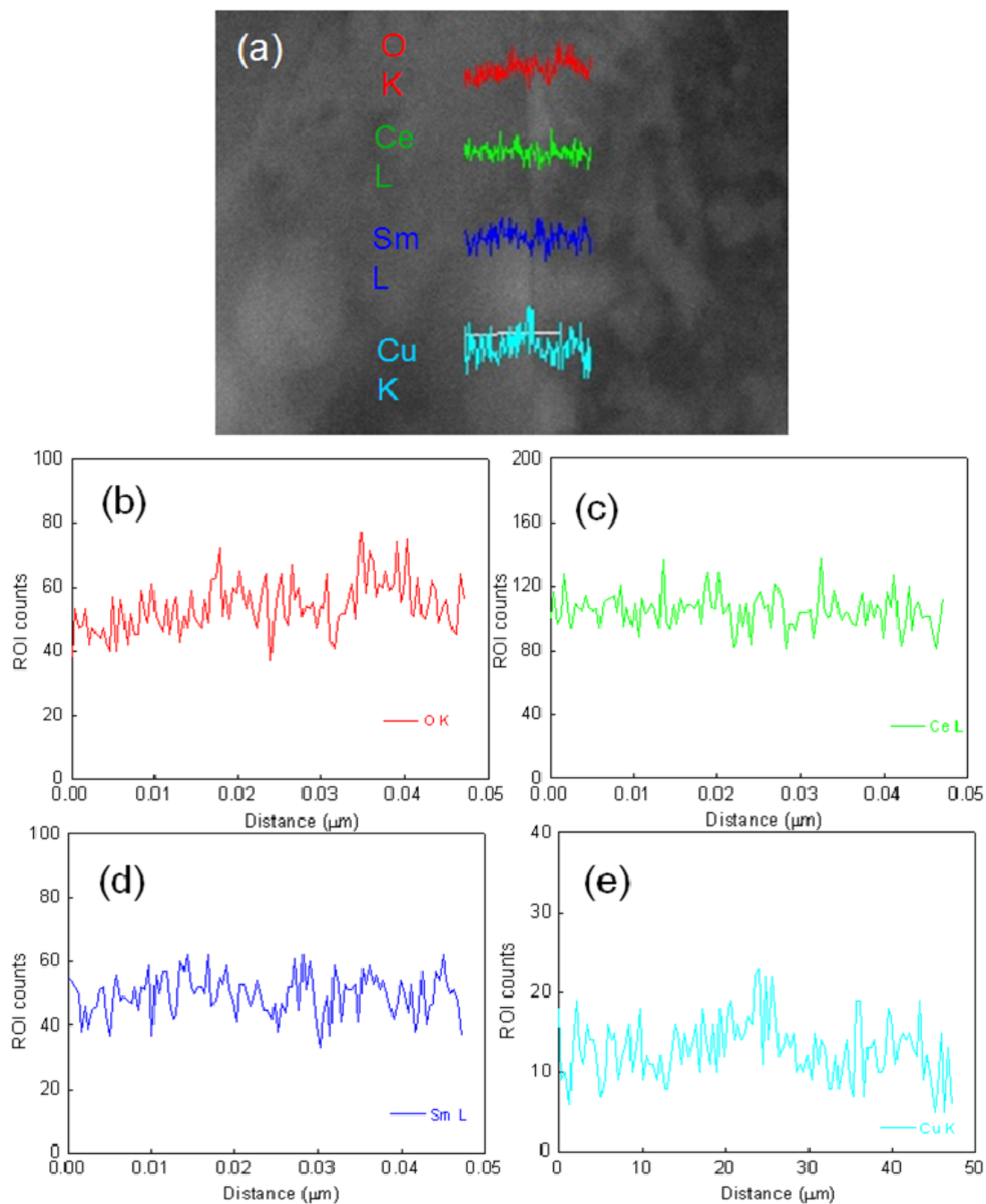


Fig. S5. STEM-EDS results for CSCO-900: (a) STEM image and EDS element linear scanning results across a binary grain boundary between two typical grains; (b) EDS element linear scanning spectrum of O (K) element; (c) EDS element linear scanning spectrum of Ce (L) element; (d) EDS element linear scanning spectrum of Sm (L) element; and (e) EDS element linear scanning spectrum of Cu (K) element.

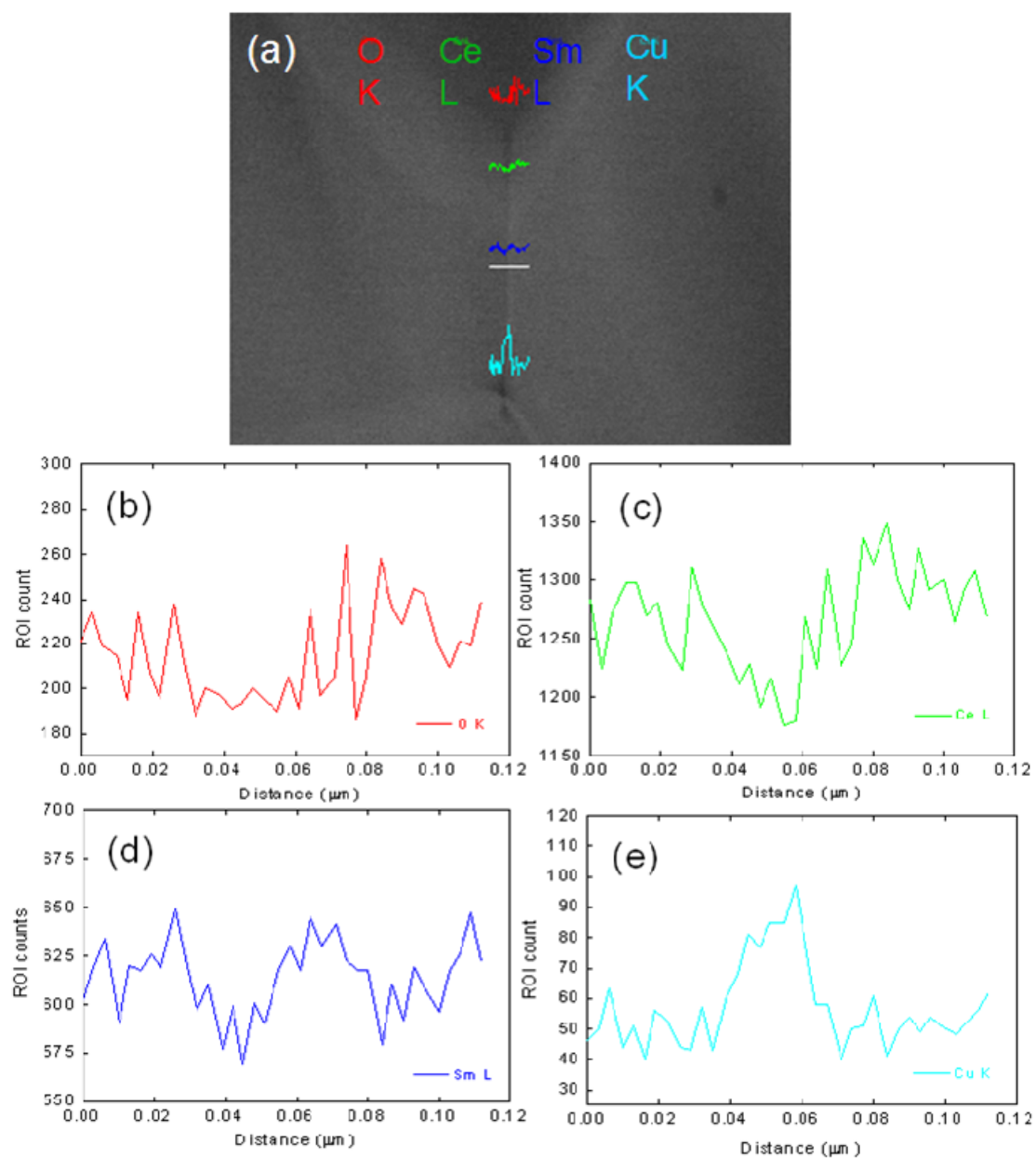


Fig. S6. STEM-EDS results for CSCO-1100: (a) STEM image and EDS element linear scanning results across a binary grain boundary between two typical grains; (b) EDS element linear scanning spectrum of O (K) element; (c) EDS element linear scanning spectrum of Ce (L) element; (d) EDS element linear scanning spectrum of Sm (L) element; and (e) EDS element linear scanning spectrum of Cu (K) element.

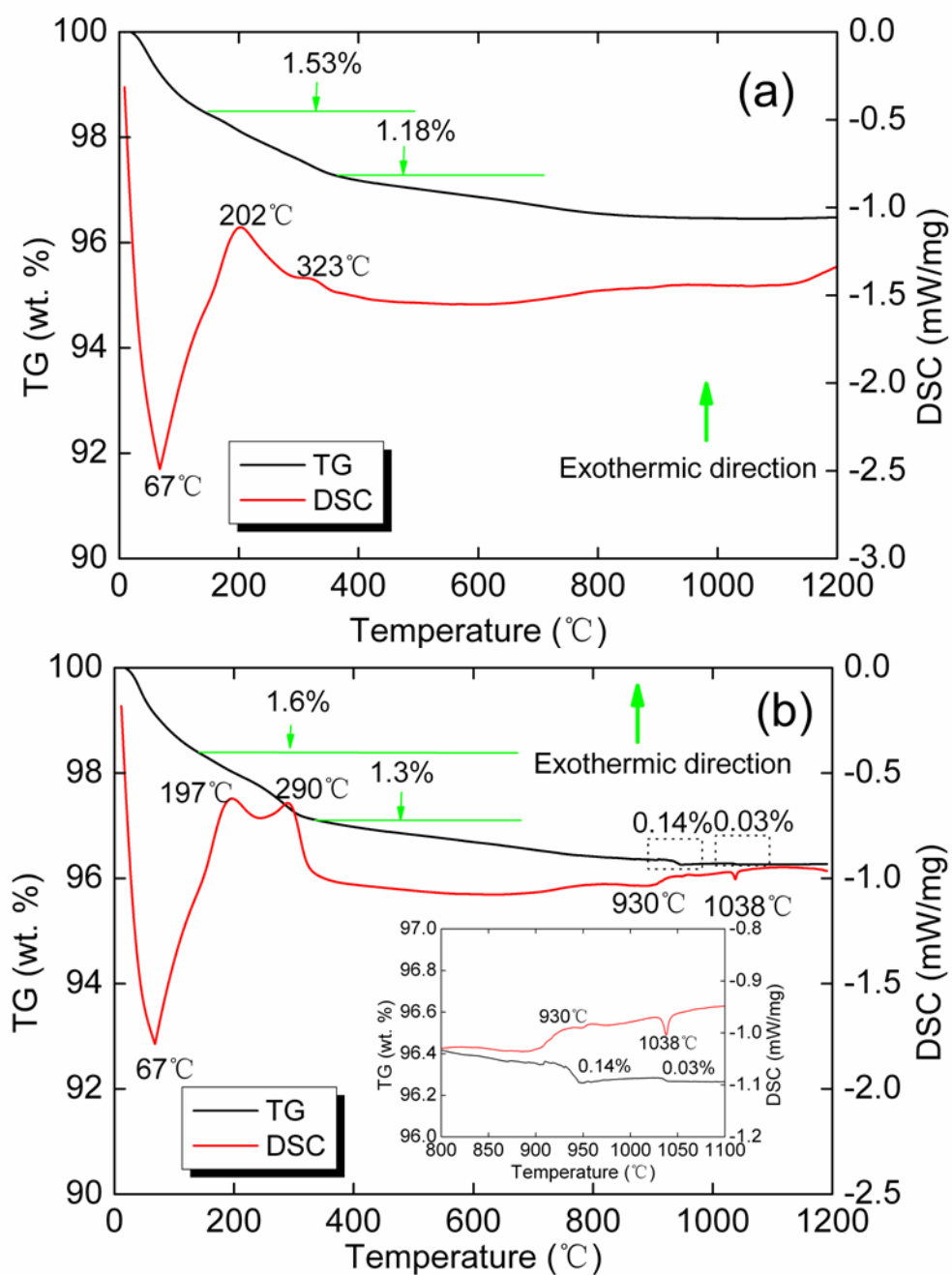


Fig. S7. TG/DSC curves of the CSO and CSCO green compacts: (a) CSO; (b) CSCO (the insert shows enlarged

TG-DSC curves ranging from 800 to 1100 °C).

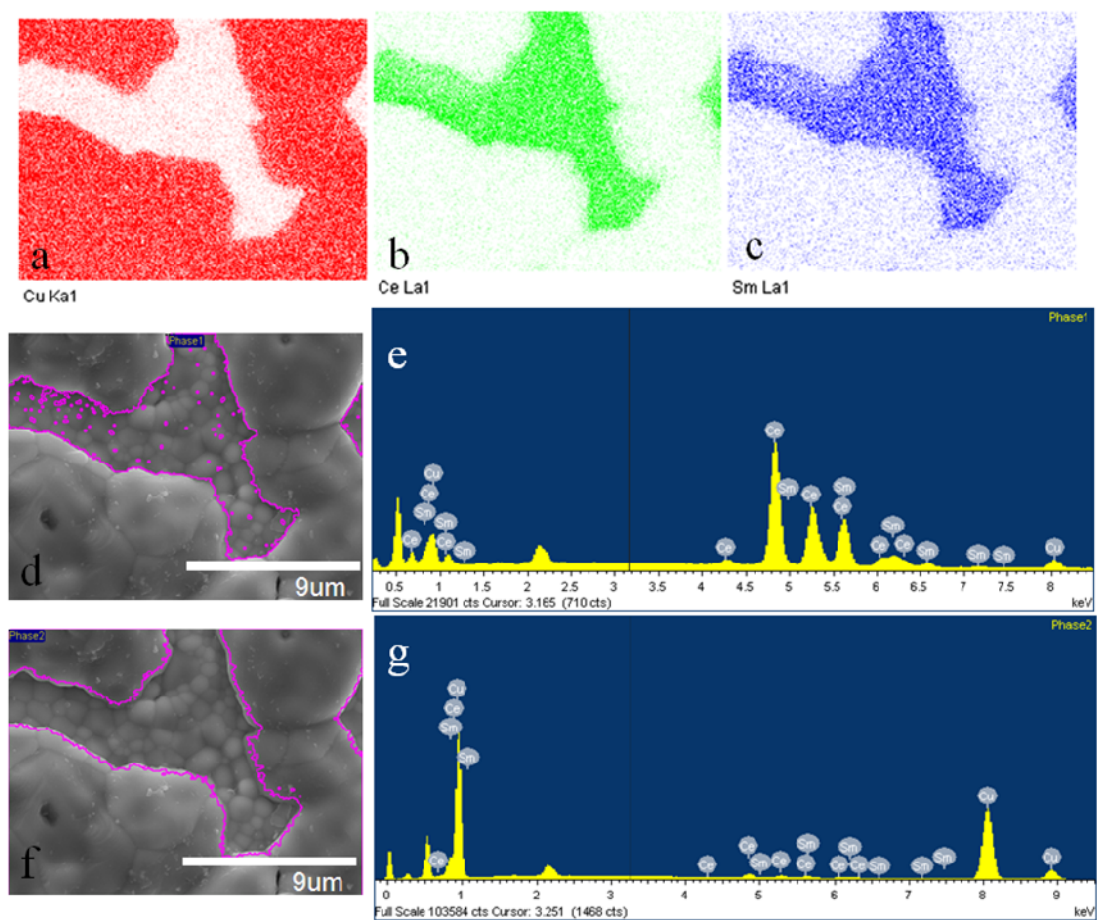


Fig. S8. SEM-EDS results for the surface of the CSCO after sintering at 1050 °C: (a) Cu element mapping; (b) Ce element mapping; (c) Sm element mapping; (d) SEM image indicating Phase-1; (e) EDS spectrum of whole Phase-1; (f) SEM image indicating Phase-2; (g) EDS spectrum of whole Phase-2.

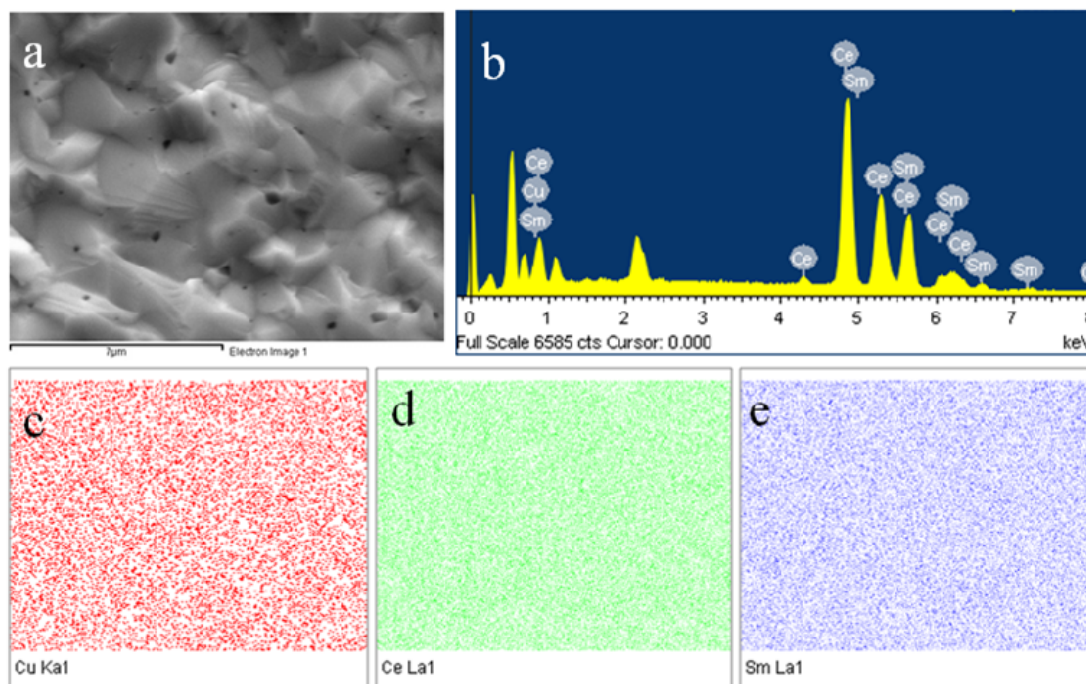


Fig. S9. SEM-EDS results for the fractural surface of the CSCO after sintering at 1050 °C: (a) SEM image; (b)

EDS spectrum of the whole SEM area; (c) Cu element mapping; (d) Ce element mapping; (e) Sm element

mapping.

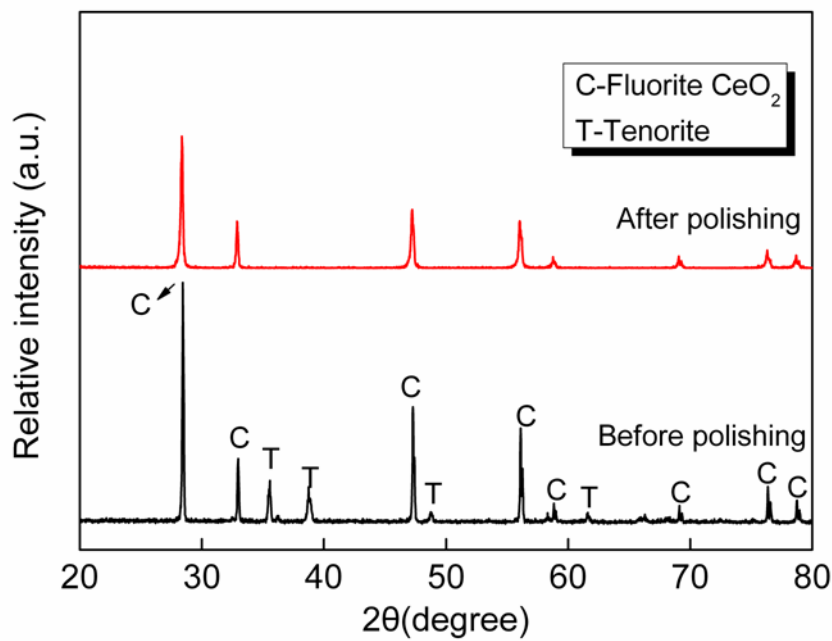


Fig. S10. XRD patterns of the CSCO-1050 samples before and after mechanical surface polishing.

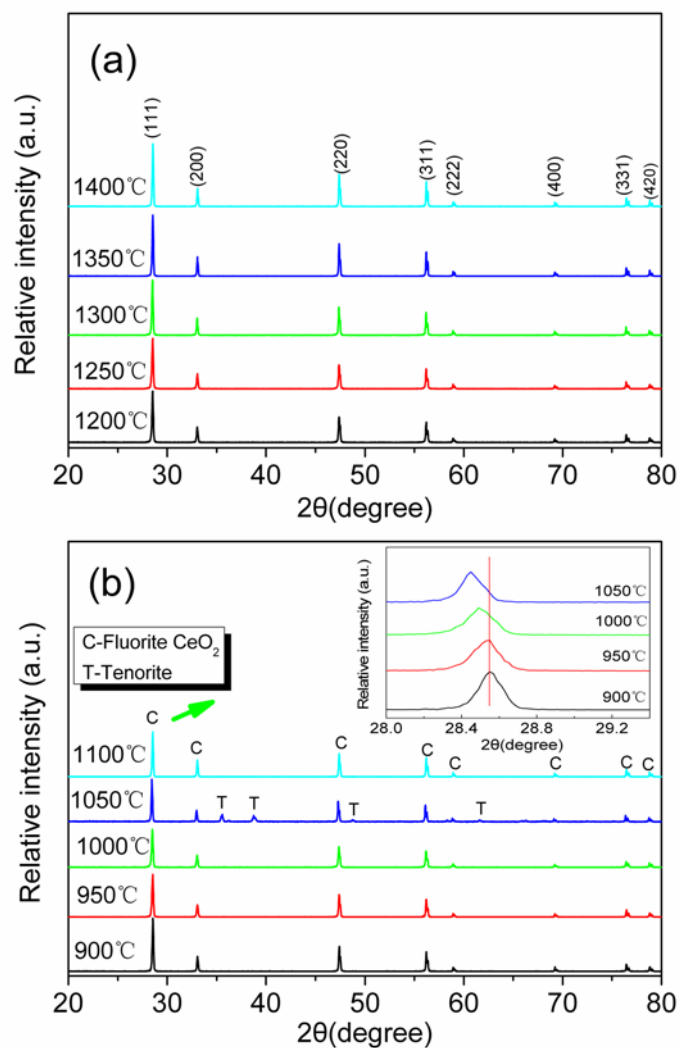


Fig. S11. XRD patterns of the CSO samples after sintering at 1200-1400 °C (a) and the CSCO samples after sintering at 900-1100 °C (b); The insert indicates the selected XRD patterns with 2θ angle ranging from 28° to

29.4°.